

# Numerical Simulation of the Aerosol Impacts on Winter Storm in Upstate New York

Yuyi Du<sup>1</sup> and Qilong Min<sup>1</sup>

<sup>1</sup>University at Albany

November 21, 2022

## Abstract

A three-day precipitation event was simulated using Weather Research and Forecasting (WRF) model coupled with a Spectral Bin Microphysical (SBM) scheme. On January 6th, a synoptic frontal system passed through NYS, and was followed by a lake effect event that lasted to January 8th, 2014. With a focus of aerosol indirect effect over the complex terrain of NYS, three sensitivity studies on this event were conducted: 1) a Control Case with background aerosol of low concentration, 2) an IN Case with doubled ice nuclei (IN) concentration, and 3) a CCN Case with tripled cloud condensate nuclei (CCN) number than the Control Case. In the frontal system, the ice-to-liquid partition within the cloud and in the surface precipitation was strongly affected by extra INs and CCNs. For the lake effect event with a much colder atmosphere, extra IN had large impact on the cloud by forming more ice crystals directly over the lake and invigorating the vertical motion within the lake effect cloud band, resulting in taller and narrower cloud band as well as increased precipitation over the downwind Tug Hill. Whereas the more numerous small cloud droplets and lower rimming efficiency associated with extra CCNs buffered the increased ice collection rate, resulting in a similar convection intensity and surface precipitation to the Control Case.

# Numerical Simulation of the Aerosol Impacts on Winter Storm in Upstate New York

Yuyi Du and Qilong Min

Atmospheric Sciences Research Center, University at Albany, Albany, NY 12237

**Correspondence:** Qilong Min (qmin@albany.edu)

## Key points:

- Numerical simulations showed that the properties of winter lake effect cloud systems were strongly affected by aerosol.
- Ice nuclei had large impact on the lake effect cloud band by forming more ice crystals directly over the lake and invigorating the vertical motion.
- More numerous small cloud droplets and lower rimming efficiency with extra cloud condensation nuclei buffered increased ice collection rate.

**Abstract:** A three-day precipitation event was simulated using Weather Research and Forecasting (WRF) model coupled with a Spectral Bin Microphysical (SBM) scheme. On January 6th, a synoptic frontal system passed through NYS, and was followed by a lake effect event that lasted to January 8th, 2014. With a focus of aerosol indirect effect over the complex terrain of NYS, three sensitivity studies on this event were conducted: 1) a Control Case with background aerosol of low concentration, 2) an IN Case with doubled ice nuclei (IN) concentration, and 3) a CCN Case with tripled cloud condensate nuclei (CCN) number than the Control Case. In the frontal system, the ice-to-liquid partition within the cloud and in the surface precipitation was strongly affected by extra INs and CCNs. For the lake effect event with a much colder atmosphere, extra IN had large impact on the cloud by forming more ice crystals directly over the lake and invigorating the vertical motion within the lake effect cloud band, resulting in taller and narrower cloud band as well as increased precipitation over the downwind Tug Hill. Whereas the more numerous small cloud droplets and lower rimming efficiency associated with extra CCNs buffered the increased ice collection rate, resulting in a similar convection intensity and surface precipitation to the Control Case.

**Key words:** aerosol-cloud interaction, lake effect, winter storm, cloud microphysics

## 1. Introduction

Aerosols affect cloud formation, morphology and lifetime, as well as precipitation intensity and distribution (e.g., Yuan et al. 2011a; Koren et al. 2012; Thompson and Eidhammer 2014), changing the radiation balance of earth (Liou et al. 1989; Albrecht 1989; Pincus and Baker 1994). The aerosol indirect effects on cloud and precipitation generally start with aerosol acting as cloud condensation nuclei (CCN) and/or ice nuclei (IN). For warm clouds that only contain liquid particles, high CCN concentration results in more numerous small droplets, increased cloud albedo and solar radiation reflection (Towmey 1977, Warren et al. 1988), cloud lifetime, cloudiness (Albrecht 1989), and suppressed warm rain (Rosenfeld 1999).

Consisting of hydrometers in both liquid and ice phase, mixed-phase clouds are

formed and maintained though more complicated macro- and micro-physical processes. Those processes are not yet completely understood theoretically and hard to fully represent in numerical models (Korolev et al. 2017). Particularly, the partition and competition between water vapor, liquid and ice water within mixed-phase clouds affects precipitation formation and cloud lifetime (Tremblay et al. 1996; Jiang et al. 2000; Korolev et al. 2003; Fan et al. 2017). Similar to warm clouds, CCN effects on mixed-phase clouds include decreased drop size (Khain et al. 2007) and increased liquid water content (Fan et al. 2012a) and both observation and modeling studies show suppressed precipitation with extra CCN (Rosenfeld 2000; Rosenfeld and Woodley 2000; Givati and Rosenfeld 2004; Jirak and Cotton 2006; Borys et al. 2000, 2003). For deep convective clouds (DCCs), CCN was shown to invigoration of the cloud by both modeling (e.g., Khain et al. 2003, 2004, 2005; Wang 2005; Lynn et al. 2005a; Teller and Levin 2006; van den Heever et al. 2006; Lee et al. 2008) and observation evidences (Koren et al. 2005). And it was reported that this invigoration effect could lead to increased surface precipitation (e.g., Ohashi and Kida 2002; Shepherd and Burian 2003; Wang 2005; Lynn et al. 2005a, b; Khain et al. 2004, 2005; Lynn et al. 2007; Tao et al. 2007). Previous studies also showed that the significance of CCN effect on convective clouds and resulted precipitation was affected by other environmental factors such as relative humidity, static stability and wind shear (e.g. Matsui et al. 2004; Khain et al. 2004, 2005, 2008, 2009; Lynn et al. 2007; Tao et al. 2007; Fan et al. 2009, 2012b).

IN enhances the heterogeneous ice formation processes in mixed-phase clouds. As a result, increased latent heat release will enhance the updraft, which carries liquid particles to higher altitude and in turn support homogeneous freezing and particle growth. This positive loop will lead to glaciation of clouds and increased surface precipitation (van den Heever et al. 2006; Yang et al. 2015). IN also results in changes in cloud morphology. Model simulation and satellite observations have shown that for DCCs, IN resulted in increased anvil coverage, cloud top temperature and stratiform precipitation (Ekman et al. 2007; Min et al. 2009; Li and Min 2010; Gibbons et al. 2018). However, Fan et al. (2017) showed that extra IN could either enhance or prohibit surface precipitation, depending on the IN, CCN concentration and cloud top temperature. Overall, it is very hard to find “climatically meaningful relationships” (Stevens and Feingold 2009) when it comes to how aerosol concentration affects precipitation systematically in the real atmosphere.

New York, the only state in the United States bordering both the Great Lakes (Erie and Ontario) and the Atlantic Ocean, features three dominant valley systems (Hudson-Champlain, Mohawk, and St. Lawrence), and two major elevated but geologically distinct regions: the Catskill Plateau (reaching up to 1100 m) in the southeast and to the north the Adirondack Mountains (maximum elevation 1629 m). Channeling within the three river valleys can extend upwards of 500 km (Freedman and Fitzjarrald 2017) and produce or exacerbate extreme and damaging winds (including tornadoes, LaPenta et al. 2005). Cold air pooling within the larger valleys and smaller, elevated valleys, presents difficulties in forecasting surface temperatures, fog appearance (Fitzjarrald and Lala 1989), air quality, and precipitation phase during snow/ice events. Lake Erie and Lake Ontario substantially influence local and regional weather and climate, presenting challenges for forecasters including lake effect snow events (Kristovich et al. 2018) and lake breeze-induced thunderstorms (Workoff et al. 2012), the contiguity features of which affect the weather and climate on multiple scales (Orlanski 1975; Fujita 1986).

Lake-, sea-, and ocean-effect events have been long recognized for bringing intense and highly localized precipitation. Such events are observed and studied by the sea located at a range of latitude (Walter 1980) and several lakes in the North America, including Lake Champlain (Laird et al. 2009), Great Salt Lake (Alcott and Steenburgh 2013), and the Great Lakes (e.g. Jiusto and Kaplan 1972; Niziol 1987; Kristovich and Steve 1995; Veals and Steenburgh 2015). For New York State (NYS), over the period of 1998 to 2018, NWS has recorded in average 10 lake effect events and over 100 inch snow accumulation over the down-wind snow belt regions of Lake Ontario and Lake Erie per year. Those frequent and intense snow events, with high records of 30.5 cm in 1 h (Burt 2007), would adversely impact local transportation, commerce, and property (Norton and Bolsenga 1993; Schmidlin 1993; Kunkel et al. 2002). Accurate predictions of lake effect events are of vital importance for weather forecasters. However, the morphology of a lake effect cloud band and its precipitation field are sensitive to surface and small scale features (Saslo and Greybush 2017), such as lake ice cover (Cordeira and Laird 2008; Gerbush et al. 2008) and complex terrain (Onton and Steenburgh 2001; Alcott and Steenburgh 2013). Improved understanding of lake effect events is necessary to diminish the uncertainty in precipitation forecasts.

Lake effect events happen when the temperature difference between lake surface and 850 mb air is larger than 13 K and the air travels over the lake surface for at least 100 km. The water vapor and energy released from the lake into the cold air will support the formation of a narrow cloud band over the lake, coupled with strong convection within the cloud band and a surface convergence zone. Recently, the Ontario Winter Lake-effect Systems (OWLeS) project was conducted over a 2-month period from December 2013 to January 2014 (Kristovich et al. 2017). Main focus of this field campaign was on the dynamics perspective of the lake band formation and precipitation. Steenburgh and Campbell (2017) pointed out that the differential surface roughness between lake and surrounding land contributed to the surface convergence, which then squeezed the temperature contours together, resulting in kinetic and diabatic frontogenesis accordingly which would promote the development of lake breeze front (LBF, a cold-warm air boundary) along the lake and therefore intensify the lake band. Apart from the frontogenesis that sustained the circulation at near surface, the latent heat release within the cloud band enhanced the vertical motion especially over the higher altitude, supporting the organization of a deep, narrow and intense cloud band (Bergmaier et al. 2017). The precipitation maximum over Tug Hill during lake effect storms has been another focus of previous studies. Apart from the six potential mechanisms summarized by Minder et al. (2015), Campbell and Steenburgh (2017) showed that a LBF along the southeast shore bulge of Lake Ontario would enhance the snow deposition and contribute to the precipitation maximum. Removal of Tug Hill led to increased sublimation rate and decreased deposition and accretion growth rate of hydrometers. However, coupled with the effect of complex terrain and diverse aerosol, the microphysics processes in lake effect cloud band formation and precipitation remain unclear and require further investigation.

From the pollution and aerosol source perspective, NYS is located in the outflow regions of major anthropogenic emissions from the Ohio River Valley Region, one of the major areas for coal-fired power generation of the United States. Part of NYS is in the middle of the Northeast Metropolitan Corridor, a very dense urban region that generates large quantities of anthropogenic emissions. Significant biogenic emissions of volatile organic carbons (VOCs) also exist in NYS, which show apparent seasonal

variations. NYS is further subject to the influence of relatively clean air masses from the southeast (ocean) and from the northern sectors (Canada). Polissar and Hopke (2001) analyzed 7-year PM<sub>2.5</sub> composition data and showed that in the Northeast, except for sulfur, anthropogenic species associated with wood burning, coal and oil combustion had higher value during the winter months. The significant spatial and temporal variability of aerosol supports that NYS is a good place to study its life cycle, interactions of anthropogenic-biogenic emissions, as well as effects of aerosol-cloud-precipitation interactions for weather systems occurring over complex terrains and influenced by mega-cities.

Several studies examined the effect of aerosol on orographic precipitation. Analysis of 50 years of rain gauge measurement showed suppressed precipitation in elevated sites that are located downwind of urban areas, along the urbanization and industrialization in California and Israel (Jirak and Cotton 2006). Model simulations agreed with the observation, showing the reduction of orographic precipitation with increased CCN concentration was a result of decreased drop size and riming efficiency (Borys et al. 2003; Saleeby et al. 2009). However, some studies pointed out the decreased riming efficiency and surface precipitation might be buffered in colder clouds, where ice crystals that grow through Wegener-Bergeron-Findeisen process played a more important role in precipitation formation (Xiao et al. 2015; Fan et al. 2017). Lynn et al. (2007) also pointed out that relative humidity and vertical velocity were able to affect the aerosol-orographic cloud interaction. Creamean et al. (2013) studied the role of IN in orographic precipitation over Sierra Nevada in California, and concluded that the increased precipitation was due to more “seeder” ice crystals formed with IN heterogeneously in the “seeder” cloud and grew into large particles in the “feeder” cloud below. However, both modeling and observational studies of IN effect are still limited. It is also worth pointed out that previous studies mainly focused on mountain regions with 3 km altitude (e.g. Sierra Nevada, the Rocky mountains, Park Range, etc.), where the forced lifting by the mountain plays an important role in cloud and precipitation formation. However, for the area of our interest, New York State, the highest elevation is the Adirondack mountain of about 1600 m, with complicated structures of hills, valleys and lakes.

In recent years, a Spectral Bin Microphysics (SBM) model coupled with the Weather Research and Forecasting (WRF) model has been employed to study the microphysics processes of various weather systems, from mid-latitude synoptic precipitation events (Fan et al. 2012a) to tropical deep convection (Gibbons et al. 2018). The original SBM model developed by Khain et al. (2004) solves a set of kinetic equations for the size distribution functions of 7 hydrometeor types: water droplets, ice crystals (plate, column, and dendrite), aggregates, graupel, and frozen drops/hail, as well as cloud condensation nuclei (CCN). Each size distribution includes 33 bins, where the mass of a particle in each bin is twice of that in the preceding bin. The fast-SBM model used in this study is modified so that the size bins are considered only for four types: water droplets, low density ice (ice crystals and aggregates), high density ice (graupel and hail), and CCN to reduce the computational costs (Khain et al. 2009). Furthermore, the ice nuclei (IN) number concentration is taken into consideration and directly linked to heterogeneous freezing (Fan et al. 2014; Gibbons et al. 2018), including deposition freezing, contact freezing and immersion freezing. The later modification provides a more accurate description especially for mixed-phase clouds. Previous model simulation from Fan et al. (2014) showed that the WRF-SBM model had good comparison with standard ground measurements such as surface precipitation as well

as microphysical measurements of cloud droplet and ice number concentration. The detailed particle formation and growth in the SBM model promotes our understanding of the microphysical processes and their influence on the microphysical-dynamical interaction over complex terrain.

In this paper, WRF-SBM model is used to study a lake effect event over Lake Ontario, focusing on the microphysical perspective in the cloud and precipitation formation processes, and its interaction with thermodynamics environments under the unique topography of New York State. Detailed experiment design is presented in section II. Simulation results are analyzed in section III. Finally, summary and conclusions are made in section IV.

## 2. Experiment design

In this study, the WRF-SBM simulations were conducted for a winter storm event, spanning from 1200UTC January 5th, 2014 to 0000UTC January 8th, 60 hours in total. Three one-way nested domains centered in the Lake Ontario and Tug Hill were used in the simulation (see Fig. 1 for the location and topography of the domains). The horizontal resolutions were 27 km, 9 km, and 3 km and the grid points were  $150 \times 150$ ,  $90 \times 90$ , and  $89 \times 89$  respectively. 56 vertical levels were from 92 m to 12300 m above sea level and the intervals were increasing with height. Initial and boundary conditions for the first domain were provided by the 6-hourly National Centers for Environmental Prediction (NCEP) global final analysis dataset with  $1^\circ \times 1^\circ$  resolution, and the initial conditions for the two inner domains were interpolated from the first domain. The SBM scheme was employed for the third domain only because it was not designed for coarse resolution. Instead, Morrison microphysics scheme (Thompson et al., 2008) was used for the domain 1 and domain 2. Other parameterizations were listed in table 1.

Three “Lake Cases” were conducted to test the aerosol effect in the event. In the Control Case, CCN and IN were set to a relatively low value to better represent the pristine environment of NYS in the winter time. The initial number concentration of CCN was set to  $300 \text{ cm}^{-3}$  and decreased exponentially with height at above 2 km altitude. The initial number concentration of IN was set to  $10 \text{ L}^{-1}$  and evenly distributed in the vertical direction. In the IN Case, a extra layer with doubled IN concentration was set between 1 km and 2 km to directly interact with the lake effect cloud band, while the CCN number concentration remained unchanged. The CCN Case tripled the CCN number concentration to represent a polluted atmosphere. The CCN and IN were advected by wind from boundaries after the simulation started to prevent dilution due to the inflow of “clean” air.

For better understanding of the land surface influence in the winter storm event, a set of “Forest (No-Lake) Cases” were conducted in contrast with the Lake Cases. In the Forest Cases, the initial CCN and IN number concentration were identical to the corresponding Lake Cases. The only difference was that in the Forest Cases, the Lake Ontario and the upstream Lake Erie were replaced with deciduous forest, the dominant land cover type in the surrounding area.

### 3. Results

#### 3.1. Event overview

This study focused on a three-day precipitation event from January 6<sup>th</sup> to January 8<sup>th</sup>, 2014 over the domain of interest. The precipitation event could be divided into two events, where the first part was a frontal system (“synoptic event”) on the 6<sup>th</sup> that brought an average of 20 mm liquid precipitation over the whole domain. The second part started from the late hours of the 6<sup>th</sup>; with the decreased surface temperature and the dominant wind shifting from south-westerly to westerly, precursors of weak lake effect cloud bands began to develop, then merged into one strong cloud band and brought snowfall mainly to the Tug Hill region on the 7<sup>th</sup> (“lake effect event”).

To assess the model performance on surface precipitation rate, University of Wyoming North Redfield Hotplate Processed and Time Series Data (Wettlaufer & Snider, 2015) was used. Fig. 2 showed the comparison between hotplate measurement with three WRF-SBM cases of the hourly precipitation rate at North redfield (43.62 °E, 75.87 °W). The model simulation produced the peak at around 12 UTC, Jan 6<sup>th</sup> with reasonably well rain rate estimation, though the timing is about 4 hours off. Comparison of radar reflectivity showed that model reproduced the cloud structure well, however, the simulated cloud is about 1 ° east to the NEXRAD measurement. The simulated lake effect event precipitation was close to the measurement, and successfully captured the increasing rain rate during the development of the cloud band in the nighttime, as well as the weakening of cloud band and precipitation intensity after the sunrise. It was also noticeable that though extra IN and CCN led to some difference in precipitation amount over North Redfield site, the difference almost disappeared after enlarging the averaging area to the whole domain.

The radar reflectivity simulator is a useful tool to evaluate model performance and is able to reduce the gap between microphysics properties in the model and standard measurements. To compare with the radar measurements, in SBM model, radar reflectivity is calculated directly based on the simulated ice, liquid and graupel particle size distribution (Gibbons et al. 2018). Using the spherical particle approximations of the Rayleigh scattering equations suggested by Ryzhkov et al. (2011), reflectivity is calculated for each mass bin and then summed over the entire size spectrum for each hydrometeor species, then combined to obtain the total reflectivity. For the lake effect event, model reflectivity simulation was compared with the in-cloud measurement by the airborne W-band Wyoming Cloud Radar (WCR) (University of Wyoming - Flight Center, 1995). Figure 3 showed the meridionally placed cross-cloud band measurement and simulation at 13:45 to 15:00 UTC, Jan 7<sup>th</sup>, with the slices moving eastwards from over the lake to over the land. The simulated reflectivity showed good comparison with radar measurements in terms of pattern and intensity, as well as provided a perk at the macro- and micro- physical properties of the cloud band. Near the start of the cloud band (Fig. 3a), the cloud band was low and narrow. As the cloud moved towards the land, it developed into a wider and deeper band with more significant convective cores (Figs. 3b, c). After the cloud band landed (Figs. 3d, e), its reflectivity achieved maximum, and the high reflectivity zone spread out and reached down to the ground. Additionally, microphysics data at flight level was collected by 2D-P PMS probes. Observation and control case

simulated PSD were averaged along the flight track at two time periods: 13:15 UTC to 16:45 UTC (Fig. 4a) and 19:15 UTC to 23:00 UTC (Fig. 4b) on January 7<sup>th</sup>. Model showed good comparison with observation for precipitation sized particles, and an underestimation for smaller particles.

### 3.2. Microphysics processes in the synoptic event

For the synoptic event, the surface temperature was at about 0 °C, and the majority of surface precipitation was in the liquid form. Most ice and snow particles had an equivalent radius (the radius of a liquid drop of the same mass) of 80~3200 μm and distributed from the surface to about 8 km, which was the -37 °C level. Liquid particles mainly accumulated at the lowest 2 km and had two major modes of about 10 μm and 500 μm (Fig. 5a), corresponding to cloud droplets and precipitable rain drops. Under the relatively warm environment, most frozen hydrometers was in the form of snow, with radius over 100 μm. Those snow particles mainly formed via heterogeneous freezing, and larger particles tended to accumulate at lower altitude (Fig. 5d).

Extra IN led to large increase in the number of ice and snow particles with radius less than 100 μm at lowest 4 km, by enhancing heterogeneous freezing and the WBF process (Fig. 5e). Under the effect of IN, more small liquid droplets were frozen by immersion and contact freezing or evaporated (Fig. 5b). The decrease in liquid droplets further resulted in a decrease in rimming efficiency. As a result of less efficient collection growth of liquid drop, concentration of large droplets with radius of several thousand micron decreased (Fig. 5b), and therefore a total decrease in liquid mixing ratio. The overall effect of IN to the cloud was that the glaciation level of the cloud descended about 2 km (Fig. 6c), agreeing well with previous studies.

Extra CCN resulted in an increase of total liquid content at almost all vertical levels (Fig. 6b, e), with a higher cloud droplet (with radius less than 10 μm) as well as a lower drizzle (with radius less than 100 μm) number and mixing ratio (Fig. 5c). The increased cloud water content resulted in increased rimming rate, whereas the decrease in size resulted in slower sedimentation of liquid particles. For the more numerous cloud droplets, some of them were transported to about 7 km altitude, and a fraction of which, with the temperature that was cold enough, formed small ice crystals by homogeneous freezing (Fig. 5f). Notice that at lowest 2 km, extra CCN resulted in a small increase of ice mixing ratio (mainly in the form of snow particles) as well as a shift from positive (increase) to negative (decrease) in liquid mixing ratio (Fig. 6d, e). This indicated that a transform occurred, where cloud droplets reacted with liquid particles and contributed to liquid content (at 1~2 km altitude), to where more cloud droplets suspended in the atmosphere and eventually reacted with IN to form ice crystals or rimmed onto snow particles at lowest 1 km (Fig. 6f). Overall, compared with the IN Case, increased CCN number left weaker impact on the cloud structure and hydrometers.

### 3.3. Microphysics processes in the lake effect event

Slices in Fig. 7 were made along the lake effect cloud band to zoom in the microphysical processes. One difference from the synoptic event was that though the lake remained ice-free and its surface temperature was above the freezing point, the temperature of air and surrounding land largely decreased. All precipitation was in the form of snow. The  $-37\text{ }^{\circ}\text{C}$  level dropped to 3 km, and homogeneous freezing became one of the major processes in the cloud and precipitation formation. For the lake effect cloud band to form, firstly, cloud droplets and snow particles began to form over the lake (Fig. 7a, g). At the beginning of the cloud formation, the vertical motion was weak (less than 0.1 m/s). Particles suspended at lowest 2 km over the lake, and spanned over a wide range in the horizontal direction in the form of three individual bands (Fig. 9a). Particles began to coalesce and grow via rimming (between small cloud droplets and ice-phase particles) and collection (between ice-phase particles) (Fig. 8a, d). During the growing process, latent heat was released, which supported the vertical motion to over 1 m/s and to a greater vertical extent (as shown in the contours in Fig 7, 8). More cloud droplets formed, hence the higher rimming rate. As a result, snow particles kept growing in number and size, bringing relatively small amount of precipitation directly over the lake (Fig. 7g, Fig. 8d). Due to the large quantity of cloud droplets ( $> 50\text{ cm}^{-3}$ ), a large number of them did not rimmed onto snow particles, but turned into small ice crystals after encountering the updraft (over 2 m/s) at  $76.2\text{ }^{\circ}\text{W}$  to  $76\text{ }^{\circ}\text{W}$  (which was where the lake-land boundary located) and was blown over the  $-37\text{ }^{\circ}\text{C}$  level, accumulating over the Tug Hill (Fig. 7d). Strong convergence could be observed at lowest 1 km as well as divergence at cloud top, over the  $-37\text{ }^{\circ}\text{C}$  level. Three weak, shallow bands from the beginning merged into one band in a tall and slender shape with the snow mixing ratio almost doubled, and a weaker band by its side (Fig. 9d). Over the land (east to the  $76\text{ }^{\circ}\text{W}$ ), ice crystals grew into snow particles by coalescence at the  $-37\text{ }^{\circ}\text{C}$  level, then began to sediment down and kept growing by rimming between 1~3 km, where ice crystals and cloud droplets were abundant, contributing to the precipitation enhancement over the Tug Hill. However, when the cloud band moved further in to the land at  $75.5\text{ }^{\circ}\text{W}$ , the cloud band became weaker due to the lack of the support from the land. Particle growth and associated latent heat release were not as strong, which combined with the downdraft associated with the downwind side of the Tug Hill, resulting in the lake band beginning to collapse into a wider shape (Fig. 9g).

Though previous studies (e.g. Fan et al., 2017) pointed out that rimming was of minor importance in winter orographic precipitation events, the unique environment in lake effect events, with the warm lake surface, the sharp vertical temperature gradient, and sufficient vapor supply, large amount of cloud droplets were able to form, (in this case, even higher than the warmer synoptic event) and were substantial to the whole lake effect event. It is noticeable that the rain drop number concentration and mixing ratio were both very low in this environment, indicating cloud droplets which did not evaporate either frozen into ice crystals or were collected by ice and snow particles. The presence of graupels and hails were negligible either, due to the lack of large rain drops.

The major difference in IN Case was that most snow particles formed as a result of ice collection growth, both directly over the lake and collocated with the ice over the Tug Hill (Fig. 7k, Fig. 8b). With extra IN, a large amount of water vapor from the lake encountered IN and nucleated into ice crystals directly, resulting in much fewer cloud droplets over the lake and accumulated over the land (Fig. 7b). Due to higher snow particle formation and growth by collection (Fig. 8b) directly over the lake and land,

stronger latent heat release enhanced the convection (Fig. 15c), and the ice collection efficiency had increased accordingly. The resulted increase of snow particle will in return enhance the latent heat release, the updraft intensity, the collection efficiency and therefore precipitation formation rate. The produced snow particles were about half the size of that in the Control Case (Fig. 8k), but were sufficient to fell out of the cloud. On the other hand, there was still water vapor transported into the updraft zone at 76 °W, formed cloud droplets and later frozen into ice. The ice mixing ratio and number concentration over Tug Hill were only slightly lower than those in the Control Case (Fig. 7b, e). The processes over the lake-land boundary could be observed in Fig. 10e, where the ‘anvil’ into the smaller size bins were narrower and the number of large particles was less than other two cases. Though rimming barely happened over the lake due to low cloud droplet concentration, and was much lower within the updraft zone compared to the Control Case (Fig. 7h), it contributed to the precipitation enhancement over Tug Hill. Adding in extra IN not only changed the microphysical processes, but also the thermodynamic structure of the cloud band. At the early stage at 77 °W, cloud bands in the IN Case had stronger vertical motion and higher snow mixing ratio, especially for the two bands to the North. The effect could be observed in Fig. 10b, where the snow number in the IN Case had increases in both at near surface for particles about 100 μm in radius, as well as smaller particles at higher altitude (about 3 km, associated with a higher cloud top). At the region where the upward motion developed to its strongest stage at 76 °W, cloud band showed a stronger vertical motion and circulation, which in turn ‘squeezed’ the cloud bands together into a single band with again higher cloud top and snow mixing ratio (Fig. 10b). The enhancement of vertical motion further extended into in-land region.

On the other hand, the macro- and microphysical processes in CCN Case was similar to the Control Case. Extra CCN resulted in the formation of more numerous and smaller cloud droplets and ice crystals, as well as higher cloud droplet and ice crystal mixing ratio (Fig. 7c, f). The decreased size slowed down the rimming rate, which offset the increased collision rate between ice particles with higher particle number concentration (Fig. 8c, f), resulting in a similar growth rate to the Control Case over Tug Hill above -37 °C level. The combined result was a similar snow number concentration, mixing ratio and therefore precipitation with the Control Case. The snow effective radius also showed that the CCN did not strongly affect the snow size and vertical distribution (Fig. 7i, l, Fig. 8f).

From the perspective of domain averaged particle size distribution (PSD), similar to the synoptic event, the snow particles outnumbered ice crystals. Liquid PSD had same two modes at 10 μm and 500 μm, while the value for larger rain drops were much lower. The system and its reaction to extra IN and CCN were similar to the synoptic event as well despite the large difference in thermodynamic environment, though the majority of hydrometers were located at below 4 km (Fig. 11a, d), corresponding to the cloud height. Extra IN resulted in an increase of small ice crystals with equivalent radius smaller than about 100 μm at about 2 km, and a decrease of larger ice particles as well as a overall decrease in liquid particles of all size (Fig. 11b, e). The results agreed well with the slices shown previously, with increased small snow particles directly over the lake, decreased ice crystal number at 4 km, and overall decrease of larger snow particles at all heights. Extra CCN resulted in increased small droplets at 2 km within the cloud band over the lake, which then homogeneously frozen into small ice crystals at higher altitude (Fig. 11c). The drizzle (with 10~100 μm radius) number decreased accordingly.

A set of sensitivity studies (“Forest (No-Lake) Cases”) where Lake Ontario and Lake Erie were replaced by forest was done to test the impact of the lakes on the thermodynamic structure and cloud band formation. During the synoptic event, similar responses were given to extra IN and CCN compared to the Lake Cases. However, for the lake effect event, replacing the lakes with forest led to a 10 K temperature decrease and much less vapor evaporated from the surface. To the south of the Lake Ontario, the 950 hPa wind field was barely affected by the presence of the lake. Convergence and divergence zone associated with the terrain around the Finger Lakes existed, the strength of which depended on the wind speed. Though no cloud formed due to the lack of water vapor. The wind field to the North of the Lake Ontario, on the other hand, had a southern orientation compared with the Forest cases, contributing to the strong convergence as part of the lake effect cloud band circulation. From the microphysics perspective, much lower liquid and ice concentration of all sizes were found in the Forest Cases (Fig. 12a, d), where small liquid particles were able to form directly with CCN but hard to grow due to low vapor pressure (Fig. 12d). The decrease in the ice number concentration was not as large as the liquid droplets, because ice requires lower vapor pressure to form and grow and deposition freezing was able to play a more important role in the Forest Cases. The lower liquid particle number did affect the homogeneous freezing rate and heterogeneous freezing where liquid particles participate (contact and immersion freezing). Apart from ice and snow formation, the lower liquid particle number limited the ability of ice particles to grow by rimming. As a result, the number of snow with equivalent radius over 500  $\mu\text{m}$  and located higher than 2 km had largely decreased.

For both Lake and Forest Cases, extra IN resulted in decreased liquid number. The decrease was smaller in the Forest Cases because the liquid number was already very low especially for droplets that had larger size and located at higher altitude, and the rimming growth of particles was inefficient. Extra IN enhanced heterogeneous freezing to form more smaller particles with radius smaller than 100  $\mu\text{m}$ , as well as suppressed homogeneous freezing at higher altitude. Extra CCN resulted in more small drops, less drizzles for the Lake Cases, and overall increase of liquid number due to little competition in the Forest Cases. Little change happened in the ice number of all sizes because the liquid number was still too low and the system was dominated by heterogeneous freezing in the Forest Cases.

### 3.4. Precipitation phase and partition

For the synoptic event, total accumulated precipitation in liquid and solid form were separated and the difference between IN, CCN and Control Case were presented in Fig. 13. As a result of increased IN number concentration, a shift of liquid particles to frozen hydrometers happened within the cloud, and the direct result was a domain-averaged 1% decrease of liquid precipitation (Fig. 13b). For the first precipitation peak that brought precipitation under the southerly wind, increased IN led to the formation of more numerous but smaller ice and snow particles that were hard to sediment and form precipitation, leading to decreased snowfall to the north of the Lake Ontario (Fig. 13e). This was because that in this precipitation process, the atmosphere was relatively warm with 0  $^{\circ}\text{C}$  level located at 2.5 km, and liquid dominated over ice. Snow mainly stayed aloft above 2 km, and liquid particle collective growth was the most important pathway in precipitation formation. A

zoom-in at lowest 2 km showed that extra IN largely affected the cloud mixing ratio and rimming rate (Fig. 14a, c), therefore snow particles had lower mixing ratio and smaller effective radius than those in the Control Case and CCN Case (Fig. 14d, e). However, for the second peak, the dominant wind shifted to southwesterly, and the atmosphere temperature decreased by 10 K (though the shape of the temperature profile had little change). Snowfall became the major type of precipitation, with few rain drops formed by near-surface melting. Cloud droplet concentration and mixing ratio were lower than the first precipitation peak, and mainly accumulated at lowest 1 km. Ice collection became the major growth method. Increased ice number in the IN Case largely increased the growth rate, and resulted in more precipitation in the Northeast corner.

Extra CCN suppressed domain-averaged liquid precipitation by 1.4%. It is noticeable that snow water equivalent (SWE) increased 4% with increased CCN number. From a closer look at the snowing region, it is noticeable that in the near surface area, the extra CCN resulted in largely increased cloud droplet mixing ratio with a slightly lower cloud droplet effect radius of about 1  $\mu\text{m}$  (Fig. 14a, b), so the rimming efficiency of a single cloud droplet will not be strongly affected. The total rimmed mass flux largely increased, and the enhanced rimming process resulted in a higher snow number concentration, mixing ratio and effective radius (Fig. 14d, e, f), and increased snowfall.

For the lake effect event, similar to the synoptic event, extra CCN resulted in a slightly increased SWE. Extra IN resulted in lower cloud droplet concentration; rimming barely happened over the lake, and snowfall over the lake was much lower (Fig. 15e). Notice that relation could be found between the latent release and surface precipitation. As stated earlier, in the IN Case, higher ice and snow particle formation and growth resulted in higher latent heat release (shown in the form of positive temperature change in Fig. 15b) over both lake and land. More particles suspended in the air and advected over the land, contributing to the enhancement over Tug Hill. The decrease in temperature, associated with the evaporation of snow particles, was lower than the Control Case, corresponding well with the decrease in accumulated precipitation (Fig. 15c, f). Fig. 15c also showed a shift in the height of positive to negative temperature change boundary (i.e. cloud base), indicating extra IN resulted in a higher cloud base. From the snowing rate perspective (Fig. 16), the cloud band shifted north and south frequently before it became relatively stationary at 08 UTC, resulted in large change in precipitation rate. Before sunrise at 12 UTC, high temperature contrast between warm lake surface and cold air resulted in strong updraft, and the enhancement due to microphysical process such as heterogeneous ice formation was relatively less important. In Control Case and CCN Case, the cloud water content was higher and rimming was sufficient, and the precipitation rates were higher. However, after sunrise, the surrounding land and air above the lake began to warm up, the temperature contrast became smaller and the microphysical invigoration of vertical motion started to play a more important role in precipitation formation. Precipitation rate in the IN Case became higher than the other two cases.

#### **4. Conclusion**

A two-day precipitation event occurred from January 5<sup>th</sup> to January 8<sup>th</sup>, 2014 over New York State. It can be divided into a synoptic event where a front system passed by and brought 20 mm precipitation mainly in the liquid form, and a lake effect event over Lake Ontario which brought snow over the downwind Tug Hill. This two-day event was simulated using WRF model coupled with a Spectral Bin Microphysical (SBM) scheme, which utilizes mass bins to track particle size rather than simple prognostic size distribution. Further modifications on the SBM scheme directly linked CCN (IN) number with droplet formation (ice heterogeneous freezing), providing a more realistic representation of cloud microphysical processes especially for mixed-phase clouds.

Previous studies of aerosol effect on orographic clouds mainly focused on mountains with about 3 km elevation, where the mountain acted as a strong dynamic forcing to the cloud and precipitation formation, and involved the seeder-feeder effect that generally occur over high mountains (e.g. Jirak and Cotton 2006; Borys et al. 2003; Saleeby et al. 2009; Xiao et al. 2015, Fan et al. 2017). Whereas this study mainly focused on NYS where the highest mountain is only about 1.5 km, and the lake effect snow, whose occurrence strongly depends on the terrain. Three sensitivity studies ('Lake Cases') were designed including a Control Case with low concentration background aerosol, a IN Case with increased IN number, and CCN Case with increased CCN. Model simulation showed good comparison with reanalysis surface precipitation and NEXRAD reflectivity in both pattern and intensity.

For the synoptic event, the partition between ice and liquid, both within the cloud and for surface precipitation, was strongly affected by adding extra IN and CCN to the environment. The synoptic event happened under a relatively warm condition, where the majority of the clouds had ice crystals coexisting with supercooled liquid droplets. With extra IN, ice formation was enhanced via deposition, contact and immersion freezing, producing large number of small ice crystals at lower altitude. The competition over available vapor between liquid and frozen hydrometers as well as IN-mediated freezing of liquid droplets resulted in lower liquid particle number concentration and mixing ratio, as well as increased ice partition within the cloud. The decreased liquid content within the cloud, especially at lower altitude, resulted in decreased surface precipitation in the form of rain. Less liquid droplets also resulted in lower rimming rate, slower snow growth and therefore lower snowfall in the IN Case under a warm, liquid-dominant environment. Though when the environment is cold enough, collective growth between ice and snow particles might counteract the decreased rimming rate, resulting in an unchanging or even higher snowfall. On the other hand, extra CCN resulted in more numerous but smaller droplets, some of which were transported upwards and frozen homogeneously at cloud top. Redistribution of vapor over increased CCN concentration suppressed drizzle formation and therefore surface rainfall. Due to the suppressed large drop formation, more cloud droplets were able to suspend in the air and reacted with snow particles. As a result, simulated surface snowfall was highest in the CCN Case.

For the lake effect event, one major difference from the synoptic event is that the environment temperature dropped; homogeneous freezing of cloud droplets became the major source for ice formation, and all precipitation was in the form of snow. Rain-sized drops barely formed, though the cloud was still in mixed phase and smaller cloud droplets played an important role in cloud initiation and precipitation formation, especially via rimming process. For the lake effect event in this study, supercool

cloud droplets and snow particles formed over the lake, then horizontally advected towards the land, during which the particles kept growing and brought small amount precipitation over the lake. Along with snow particles, remaining droplets encountered the lake breeze front previously pointed out by Campbell and Steenburgh (2017), and were blew to over 3 km to be frozen into ice crystals. The ice crystals grew into snow particles by rimming and coalescence, and eventually large enough to sediment down, snow particles further increase in size by rimming with cloud droplets, contributing to the precipitation enhancement over the Tug Hill.

IN and CCN effect were closely examined to study the aerosol-cloud interaction under the complex terrain in lake effect events. It was found that with extra IN, a part of vapor and cloud droplets from the lake directly deposited onto or reacted with IN to form ice crystals, resulted in lower cloud droplet number and mixing ratio over the lake. The more active ice formation and collection over the lake led to higher latent heat release that would enhance the convective updraft, resulting in less precipitation over the lake and stronger advection of hydrometers eastwards and upwards. The stronger updraft and associated circulation resulted in a higher cloud top and snow mixing ratio. The decrease of cloud droplet number did affect the rimming rate, and resulted in smaller snow effective radius, though ice collection rate increased due to higher number of ice crystals. As a result, the precipitation in the IN Case was lower over the lake and higher over the Tug Hill. In the CCN Case, larger number of cloud droplets turned into higher number of ice crystals over land by homogeneous freezing, and eventually higher collection growth rate. On the other hand, the decreased droplet size lowered the rimming efficiency. The combined result was a similar microphysical properties and surface precipitation rate and accumulation, to the Control Case.

Lake Ontario and Lake Erie were replaced by forest in the No-Lake (Forest) Cases to better understand how lakes interact with the thermodynamic environment and cloud processes. During the synoptic event, the lake Cases and No-Lake Cases gave similar response to extra IN and CCN, indicating that the land surface had small impact on the synoptic event in this study. However, for the lake effect event, the atmosphere became dryer, colder and more stable. Removal of the lake not only affected the cloud formation due to lake of vapor and heat, but also changes in the wind field. Adding extra IN resulted in decreased liquid number that was already very low, and higher ice number for lower altitude due to more active heterogeneous freezing. Extra CCN resulted in overall increase of liquid number and little change in ice spectrum.

**Acknowledgments and Data:** This work was supported by the NSF under contracts AGS-1608735 and PIRE-1545917, the NOAA Educational Partnership Program under agreement No. #NA16SEC4810006, and by the U.S. Department of Energy Office of Energy Efficiency and Renewable Energy Solar Energy Technologies Office (#33504). WRF-ARW model (version 3) is available at <https://www2.mmm.ucar.edu/wrf/users/> (doi:10.5065/D68S4MVH). NCEP FNL Analyses can be found at <https://rda.ucar.edu/datasets/ds083.2/> (doi:10.5065/D6M043C6). NEXRAD data is available at <https://www.ncdc.noaa.gov/nexradinv/> (doi:10.7289/V5W9574V). And University of Wyoming King Air Research data can be downloaded from their website <http://flights.uwyo.edu/projects/owles13/>.

## 5. References

- Ackerman, A. S., M. P. Kirkpatrick, D. E. Stevens, and O. B. Toon, 2004: The impact of humidity above stratiform clouds on indirect aerosol climate forcing. *Nature*, 432, 1014–1017, doi:10.1038/nature03174.
- Albrecht, B. A., 1989: Aerosols, cloud microphysics and fractional cloudiness. *Science* 245, 1227–1230 (1989)
- Alcott, T. I., and W. J. Steenburgh, 2013: Orographic Influences on a Great Salt Lake–Effect Snowstorm. *Mon. Wea. Rev.* 141, 2432–2450, DOI: 10.1175/MWR-D-12-00328.1
- Andreae, M. O., D. Rosenfeld, P. Artaxo, A. A. Costa, G. P. Frank, K. M. Longo, and M. A. Silva-Dias, 2004: Smoking rain clouds over the Amazon. *Science*, 303, 1337–1342, doi:10.1126/science.1092779.
- Asai, T., and Y. Miura, 1981: An analytical study of meso-scale vortex-like disturbances observed around Wakasa Bay area. *J. Meteorol. Soc. Jpn.* 59, 832–843.
- Bergeron, T., 1935: On the physics of clouds and precipitation. *Proces Verbaux de l'Association de Météorologie, International Union of Geodesy and Geophysics*, 156–178.
- Borys, R. D., D. H. Lowenthal, and D. L. Mitchell, 2000: The relationships among cloud microphysics, chemistry, and precipitation rate in cold mountain clouds. *Atmos. Environ.*, 34, 2593–2602.
- Borys, R. D., D. H. Lowenthal, S. A. Cohn, and W. O. Brown, 2003: Mountaintop and radar measurements of anthropogenic aerosol effects on snow growth and snowfall rate, *Geophys. Res. Lett.*, 30(10), 1538, doi:10.1029/2002GL016855.
- Burt, C. C., 2007: *Extreme Weather: A Guide & Record Book*. W. W. Norton, 304 pp.
- Chen, Y.-C., M. W. Christensen, D. J. Diner, and M. J. Garay, 2015: Aerosol-cloud interactions in ship tracks using Terra MODIS/MISR. *J. Geophys. Res. Atmos.*, 120, 2819–2833, doi:10.1002/2014JD022736.
- Christensen, M. W., and G. L. Stephens, 2011: Microphysical and macrophysical responses of marine stratocumulus polluted by underlying ships: Evidence of cloud deepening. *J. Geophys. Res.*, 116, D03201, doi:10.1029/2010JD014638.
- Christensen, M. W., and G. L. Stephens, 2012: Microphysical and macrophysical responses of marine stratocumulus polluted by underlying ships: 2. Impacts of haze on precipitating clouds. *J. Geophys. Res.*, 117, D11203, doi:10.1029/2011JD017125.
- Cordeira, J. M., and N. F. Laird, 2008: The influence of ice cover on two lake-effect snow events over Lake Erie. *Mon. Wea. Rev.*, 136, 2747–2763, doi:10.1175/2007MWR2310.1.
- Creamean, J. M., Suski, K. J., Rosenfeld, D., Cazorla, A., DeMott, P. J., Sullivan, R. C., White, A. B., Ralph F. M., Minnis P., Comstock, J. M., Tomlinson, J. M., and Prather, K. A., 2013: Dust and Biological Aerosols from the Sahara and Asia Influence Precipitation in the Western US, *Science*, 339, 1572–1578, doi:10.1126/science.1227279.
- Ekman, A. M. L., A. Engstrom, and C. Wang, 2007: The effect of aerosol composition and concentration on the development and anvil properties of a continental deep convective cloud. *Quart. J. Roy. Meteor. Soc.*, 133, 1439–1452, doi:10.1002/qj.108.
- Fan, J., and Coauthors, 2009: Dominant role by vertical wind shear in regulating aerosol effects on deep convective clouds. *J. Geophys. Res.*, 114, D22206, doi:10.1029/2009JD012352.

- Fan, J., L. R. Leung, Z. Li, H. Morrison, H. Chen, Y. Zhou, Y. Qian, and Y. Wang, 2012a: Aerosol impacts on clouds and precipitation in eastern China: Results from bin and bulk microphysics. *J. Geophys. Res.*, 117,D00K36, doi:10.1029/2011JD016537.
- Fan, J., D. Rosenfeld, Y. Ding, L. R. Leung, and Z. Li, 2012b: Potential aerosol indirect effects on atmospheric circulation and radiative forcing through deep convection. *Geophys. Res. Lett.*, 39, L09806, doi:10.1029/2012GL051851.
- Fan, J., L. R. Leung, D. Rosenfeld, and P. J. DeMott, 2017: Effects of cloud condensation nuclei and ice nucleating particles on precipitation processes and supercooled liquid in mixed-phase orographic clouds. *Atmos. Chem. Phys.*, 17, 1017–1035, doi:10.5194/acp-17-1017-2017.
- Feingold, G., H. Jiang, and J. Y. Harrington, 2005: On smoke suppression of clouds in Amazonia. *Geophys. Res. Lett.*, 32, L02804, doi:10.1029/2004GL021369.
- Findeisen, W., 1938: Kolloid-meteorologische Vorgänge bei Neiderschlagsbildung. *Meteor. Z.*, 55, 121–133.
- Fitzjarrald, D. R. and G. Garland Lala, 1989: Hudson Valley Fog Environments. *J. of Appl. Meteor.*, 28, 1303-1328, [https://doi.org/10.1175/1520-0450\(1989\)028<1303:HVFE>2.0.CO;2](https://doi.org/10.1175/1520-0450(1989)028<1303:HVFE>2.0.CO;2)
- Freedman, J. M. and D. R. Fitzjarrald, 2017: Mechanisms Responsible for the Observed Thermodynamic Structure in a Convective Boundary Layer Over the Hudson Valley of New York State. *Boundary-Layer Meteorol.*, 164:89–106, DOI 10.1007/s10546-017-0241-6
- Fujita, T. T., 1986: Mesoscale Classifications: Their History and Their Application to Forecasting. *Mesoscale Meteorology and Forecasting*, pp 18-35.
- Gerbush, M. R., D. A. R. Kristovich, and N. F. Laird, 2008: Mesoscale boundary layer and heat flux variations over pack ice covered Lake Erie. *J. Appl. Meteor. Climatol.*, 47, 668–682, doi:10.1175/2007JAMC1479.1.
- Gibbons, M., Q. Min, and J. Fan, 2018: Investigating the impacts of Saharan dust on tropical deep convection using spectral bin microphysics. *Atmos. Chem. Phys.*, 18, 12161-12184, <https://doi.org/10.5194/acp-18-12161-2018>
- Givati, A., and D. Rosenfeld, 2004: Quantifying precipitation suppression due to air pollution. *J. Appl. Meteor.*, 43, 1038–1056.
- Holroyd, E. W., 1971: Lake-effect cloud bands as seen from weather satellites. *J. Atmos. Sci.*, 28, 1165–1170, doi:10.1175/1520-0469(1971)028,1165:LECBAS.2.0.CO;2.
- Jiang, H., Cotton, W. R., Pinto, J. O., Curry, J. A. and Weissbluth, M. J., 2000: Cloud resolving simulations of mixed-phase Arctic stratus observed during BASE: sensitivity to concentration of ice crystals and large-scale heat and moisture advection. *J. Atmos. Sci.*, 57, 2105–2117
- Jirak, I. L., and W. R. Cotton, 2006: Effect of air pollution on precipitation along the front range of the Rocky Mountains. *J. Appl. Meteor. Climatol.*, 45, 236–245.
- Justo, J. E., and M. L. Kaplan, 1972: Snowfall from lake effect storms. *Mon. Wea. Rev.*, 100, 62–66, doi:10.1175/1520-0493(1972)100,0062:SFLS.2.3.CO;2.
- Kain, J. S.: The Kain-Fritsch convective parameterization: an update, *J. Appl. Meteorol.*, 43, 170–181, 2004.
- Khain, A. P., D. Rosenfeld, and A. Pokrovsky, 2003: Simulation of aerosol effects on convective clouds developed under continental and maritime conditions. *Geophysical Research Abstracts*, Vol. 5, Abstract 03180.

- Khain, A. P., and A. Pokrovsky, 2004: Simulation of effects of atmospheric aerosols on deep turbulent convective clouds using a spectral microphysics mixed-phase cumulus cloud model. Part II: Sensitivity study. *J. Atmos. Sci.*, 61, 2983–3001.
- Khain, A. P., A. Pokrovsky, M. Pinsky, A. Seifert, and V. Phillips, 2004: Simulation of effects of atmospheric aerosols on deep turbulent convective clouds using a spectral microphysics mixed-phase cumulus cloud model. Part I: Model description. *J. Atmos. Sci.*, 61, 2963–2982.
- Khain, A. P., D. Rosenfeld, and A. Pokrovsky, 2005: Aerosol impact on the dynamics and microphysics of deep convective clouds. *Quart. J. Roy. Meteor. Soc.*, 131, 2639–2663.
- Khain, A. P., N. BenMoshe, and A. Pokrovsky, 2008: Factors determining the impact of aerosols on surface precipitation from clouds: An attempt at classification. *J. Atmos. Sci.*, 65, 1721–1748, doi:10.1175/2007JAS2515.1.
- Khain, A. P., L. R. Leung, B. Lynn, and S. Ghan, 2009: Effects of aerosols on the dynamics and microphysics of squall lines simulated by spectral bin and bulk parameterization schemes. *J. Geophys. Res.*, 114, D22203, doi:10.1029/2009JD011902.
- Koren, I., Y. J. Kaufman, D. Rosenfeld, L. A. Remer, and Y. Rudich, 2005: Aerosol invigoration and restructuring of Atlantic convective clouds. *Geophys. Res. Lett.*, 32, L14828, doi:10.1029/2005GL023187.
- Koren, I., L. A. Remer, O. Altaratz, J. V. Martins, and A. Davidi, 2010: Aerosol-induced changes of convective cloud anvils produce strong climate warming. *Atmos. Chem. Phys.*, 10, 5001–5010, doi:10.5194/acp-10-5001-2010.
- Koren, I., O. Altaratz, L. A. Remer, G. Feingold, J. V. Martins, and R. H. Heiblum, 2012: Aerosol-induced intensification of rain from the tropics to the mid-latitudes. *Nat. Geosci.*, 5, 118–122, doi:10.1038/ngeo1364.
- Korolev, A. V., G. A. Isaac, S. G. Cober, J. W. Strapp, and J. Hallett, 2003: Microphysical characterization of mixed-phase clouds. *Q. J. R. Meteorol. Soc.*, 129, 39–65, doi:10.1256/qj.01.204
- Korolev, A., G. McFarquhar, P. R. Field, C. Franklin, P. Lawson, Z. Wang, E. Williams, S. J. Abel, D. Axisa, S. Borrmann, J. Crosier, J. Fugal, M. Krämer, U. Lohmann, O. Schlenker, M. Schnaiter, and M. Wendisch, 2017: Mixed-Phase Clouds: Progress and Challenges. *Meteorological Monographs*, 58, 5.1–5.50, doi:10.1175/AMSMONOGRAPHS-D-17-0001.1
- Kristovich, D. A. R., and R. A. Steve, 1995: A satellite study of cloud-band frequencies of the Great Lakes. *J. Appl. Meteor.*, 34, 2083–2090, doi:10.1175/1520-0450(1995)034<2083:ASSOCB.2.0.CO;2.
- Kristovich, D. A. R., L. Bard, L. Stoecker and B. Geerts, 2018: Influence of Lake Erie on a Lake Ontario Lake-Effect Snowstorm. *J. Appl. Meteorol. Climatol.*, 57, 2019–2033, <https://doi.org/10.1175/JAMC-D-17-0349.1>
- Kunkel, K. E., N. E. Westcott, and D. A. R. Kristovich, 2002: Effects of climate change on heavy lake-effect snowstorms near Lake Erie. *J. Great Lakes Res.*, 28, 521–536, doi:10.1016/S0380-1330(02)70603-5.
- Laird, N. F., J. Desrochers, and M. Payer, 2009: Climatology of lake-effect precipitation events over Lake Champlain. *J. Appl. Meteorol. Climatol.* 48, 232–250.
- LaPenta, K. D., L. F. Bosart, T. J. Galarneau Jr., and M. J. Dickinson, 2005: A Multiscale Examination of the 31 May 1998 Mechanicville, New York, Tornado. *Weather and Forecasting*, 20, 494–516, <https://doi.org/10.1175/WAF875.1>
- Lavoie, R. L., 1972: A mesoscale numerical model of lake-effect storms. *J. Atmos. Sci.*, 29, 1025–1040, doi:10.1175/1520-0469(1972)029<1025:AMNMOL.2.0.CO;2.

- Lee, S., L. Donner, and V. Phillips, 2008: Impact of aerosols on precipitation in deep convection. *Q. J. R. Meteorol. Soc.* 134: 1201–1220, DOI: 10.1002/qj.287
- Li, R., and Q.-L. Min, 2010: Impacts of mineral dust on the vertical structure of precipitation. *J. Geophys. Res.*, 115, D09203, doi:10.1029/2009JD011925.
- Li, Z., F. Niu, J. Fan, Y. Liu, D. Rosenfeld, and Y. Ding, 2011: Longterm impacts of aerosols on the vertical development of clouds and precipitation. *Nat. Geosci.*, 4, 888–894, doi:10.1038/ngeo1313.
- Liou, K.-N. & Ou, S.-C., 1989: The role of cloud microphysical processes in climate: an assessment from a one-dimensional perspective. *J. Geophys. Res.*, 94, 8599–8607.
- Lohmann, U., 2002: A glaciation indirect aerosol effect caused by soot aerosols. *Geophysical Research Letters*, 29(4), 1052. <https://doi.org/10.1029/2001GL014357>
- Lynn, B. H., A. Khain, J. Dudhia, D. Rosenfeld, A. Pokrovsky, and A. Seifert, 2005a: Spectral (bin) microphysics coupled with a mesoscale model (MM5). Part I: Model description and first results. *Mon. Wea. Rev.*, 133, 44–58.
- Lynn, B. H., A. Khain, J. Dudhia, D. Rosenfeld, A. Pokrovsky, and A. Seifert, 2005b: Spectral (bin) microphysics coupled with a mesoscale model (MM5). Part II: Simulation of a CaPE rain event with squall line. *Mon. Wea. Rev.*, 133, 59–71.
- Lynn, B. H., A. Khain, D. Rosenfeld, and W. Woodley, 2007: Effects of aerosols on precipitation from orographic clouds. *J. Geophys. Res.*, 112, D10225, doi:10.1029/2006JD007537.
- the climate system. *Geophysical Research Letters*, 31, L06109. <https://doi.org/10.1029/2003GL019287>
- Matsui, T., Masunaga, H., Pielke, R. A. S., & Tao, W. K. (2004). Impact of aerosols and atmospheric thermodynamics on cloud properties within the climate system. *Geophysical Research Letters*, 31, L06109. <https://doi.org/10.1029/2003GL019287>
- Matsui, T., Masunaga, H., Pielke, R. A. S., & Tao, W. K. (2004). Impact of aerosols and atmospheric thermodynamics on cloud properties within the climate system. *Geophysical Research Letters*, 31, L06109. <https://doi.org/10.1029/2003GL019287>
- Masunaga, H., Pielke, R. A. S., & Tao, W. K. (2004). Impact of aerosols and atmospheric thermodynamics on cloud properties within the climate system. *Geophysical Research Letters*, 31, L06109. <https://doi.org/10.1029/2003GL019287>
- Masunaga, H., Pielke, R. A. S., & Tao, W. K. (2004). Impact of aerosols and atmospheric thermodynamics on cloud properties within the climate system. *Geophysical Research Letters*, 31, L06109. <https://doi.org/10.1029/2003GL019287>
- Matsui, T., Masunaga, H., Pielke, R. A. S., & Tao, W. K., 2004: Impact of aerosols and atmospheric thermodynamics on cloud properties within the climate system. *Geophysical Research Letters*, 31, L06109. <https://doi.org/10.1029/2003GL019287>
- Min, Q.-L., R. Li, B. Lin, E. Joseph, S. Wang, Y. Hu, V. Morris, and F. Chang, 2009: Evidence of mineral dust altering cloud microphysics and precipitation. *Atmos. Chem. Phys.*, 9, 3223–3231, doi:10.5194/acp-9-3223-2009.
- Nakai, S., K. Iwanami, R. Misumi, S. G. Park, and T. Kobayashi, 2005: A classification of snow clouds by Doppler radar observations at Nagaoka, Japan. *Sci. Online Lett. Atmos.* 1, 161–164.

- Nakanishi, M. and Niino, H., 2008: An improved Mellor–Yamada level-3 model: Its numerical stability and application to a regional prediction of advection fog, *Bound.-Lay. Meteorol.*, 119, 397–407.
- National Centers for Environmental Prediction/National Weather Service/NOAA/U.S. Department of Commerce: NCEP FNL Operational Model Global Tropospheric Analyses, continuing from July 1999, Research Data Archive at the National Center for Atmospheric Research, Computational and Information Systems Laboratory, Boulder, Colorado, available at: <https://doi.org/10.5065/D6M043C6> (last access: 1 April 2020), 2000.
- Niu, F., and Z. Li, 2012: Systematic variations of cloud top temperature and precipitation rate with aerosols over the global tropics. *Atmos. Chem. Phys.*, 12, 8491–8498, doi:10.5194/acp-12-8491-2012.
- Niziol, T. A., 1987: Operation forecasting of lake effect snowfall in western and central New York. *Wea. Forecasting*, 2, 310–321, doi:10.1175/1520-0434(1987)002,0310:OFOLES.2.0.CO;2.
- NOAA National Weather Service (NWS) Radar Operations Center (1991): NOAA Next Generation Radar (NEXRAD) Level 2 Base Data. [Product: Base Reflectivity]. NOAA National Centers for Environmental Information. doi:10.7289/V5W9574V [last accessed: April 1st, 2020].
- Norton, D. C., and S. J. Bolsenga, 1993: Spatiotemporal trends in lake effect and continental snowfall in the Laurentian Great Lakes, 1951–1980. *J. Climate*, 6, 1943–1956, doi:10.1175/1520-0442(1993)006,1943:STILEA.2.0.CO;2.
- Ohashi, Y., and H. Kida, 2002: Local circulations developed in the vicinity of both coastal and inland urban areas: A numerical study with a mesoscale atmospheric model. *J. Appl. Meteor.*, 41, 30–45.
- Onton, D. J., and W. J. Steenburgh, 2001: Diagnostic and sensitivity studies of the 7 December 1998 Great Salt Lake-effect snowstorm. *Mon. Wea. Rev.*, 129, 1318–1388, doi:10.1175/1520-0493(2001)129,1318:DASSOT.2.0.CO;2.
- Orlanski, I., 1975: A rational subdivision of scales for atmospheric processes. *Bull. Amer. Meteor. Soc.*, 56, 527–530.
- Pincus, R. & M. B. Baker, 1994: Effect of precipitation on the albedo susceptibility of clouds in the marine boundary layer. *Nature*, 372, 250–252.
- Polissar, A. V., Hopke, P. K., Poirot, R. L., 2001: Atmospheric aerosol over Vermont: chemical composition and sources. *Environ. Sci. Technol.*, 35(23), 4604–4621, doi: 10.1021/es0105865.
- Rosenfeld, D., 2000: Suppression of rain and snow by urban and industrial air pollution. *Science*, 287, 1793–1796.
- Rosenfeld, D., and W. L. Woodley, 2000: Deep convective clouds with sustained supercooled liquid water down to -37.5°C. *Nature*, 405, 440–442.
- Saleeby, S. M., W. R. Cotton, D. Lowenthal, R. D. Borys and M. A. Wetzal, 2009: Influence of Cloud Condensation Nuclei on Orographic Snowfall, *J. Appl. Meteorol. Clim.*, 48, 903–922, DOI: 10.1175/2008JAMC1989.1
- Saslo, S. and S.J. Greybush, 2017: Prediction of Lake-Effect Snow Using Convection-Allowing Ensemble Forecasts and Regional Data Assimilation. *Wea. Forecasting*, 32, 1727–1744, <https://doi.org/10.1175/WAF-D-16-0206.1>
- Schmidlin, T. W., 1993: Impacts of severe winter weather during December 1989 in the Lake Erie snowbelt. *J. Climate*, 6, 759–767, doi:10.1175/1520-0442(1993)006,0759:IOSWWD.2.0.CO;2.
- Shepherd, J. M., and S. J. Burian, 2003: Detection of urban-induced rainfall anomalies in a major coastal city. *Earth Interactions*, 7. [Available online at <http://EarthInteractions.org/>]

Skamarock, W. C., Klemp, J. B., Dudhia, J., Gill, D. O., Barker, D. M., Duda, M., and Powers, J. G., 2008: A Description of the Advanced Research WRF Version 3 NCAR Technical Note, Boulder, CO.

Smirnova, T. G., Brown, J. M., and Benjamin, S. G., 1997: Performance of different soil model configurations in simulating ground surface temperature and surface fluxes, *Mon. Weather Rev.*, 125, 1870–1884, [https://doi.org/10.1175/1520-0493\(1997\)125<1870:PODSMC>2.0.CO;2](https://doi.org/10.1175/1520-0493(1997)125<1870:PODSMC>2.0.CO;2)

Stamnes, K., et al., 1988: Numerically stable algorithm for discreteordinate-method radiative transfer in multiple scattering and emitting layered media, *Appl. Opt.*, 27(12), 2502–2509, doi:10.1364/AO.27.002502

Stevens, B., & Feingold, G., 2009: Untangling aerosol effects on clouds and precipitation in a buffered system. *Nature*, 461, 607-613.

Tao, W.-K., X. Li, A. Khain, T. Matsui, S. Lang, and J. Simpson, 2007: The role of atmospheric aerosol concentration on deep convective precipitation: Cloud-resolving model simulations. *J. Geophys. Res.*, 112, D24S18, doi:10.1029/2007JD008728.

Teller, A., and Z. Levin, 2006: The effects of aerosols on precipitation and dimensions of subtropical clouds: A sensitivity study using a numerical cloud model. *Atmos. Chem. Phys.*, 6, 67–80.

Thompson, G., and T. Eidhammer, 2014: A study of aerosol impacts on clouds and precipitation development in a large winter cyclone. *J. Atmos. Sci.*, 71, 3636–3658, doi:10.1175/JAS-D-13-0305.1.

Tremblay, A., Glazer, A., Benoit, W. and Yu, R., 1996: A mixed-phase cloud scheme based on a single prognostic equation. *Tellus.*, 48, 483–500.

Tsuboki, K., Y. Fujiyoshi, and G. Wakahama, 1989: Structure of land breeze and snowfall enhancement at the leading edge. *J. Meteorol. Soc. Jpn.* 67, 757–770.

Twomey, S., 1977: Influence of pollution on shortwave albedo of clouds. *J. Atmos. Sci.*, 34, 1149–1152, doi:10.1175/1520-0469(1977)034,1149:TIOPOT.2.0.CO;2.

University of Wyoming - Flight Center, 1995: University of Wyoming Cloud Radar (WCR). University of Wyoming, College of Engineering, Department of Atmospheric Science, doi:10.15786/M2237S.

van den Heever, S. C., G. G. Carrio, W. R. Cotton, P. J. DeMott, and A. J. Prenni, 2006: Impacts of nucleating aerosol on Florida storms. Part I: Mesoscale simulations. *J. Atmos. Sci.*, 63, 1752–1775, doi:10.1175/JAS3713.1.

Veals, P. G., and W. J. Steenburgh, 2015: Climatological characteristics and orographic enhancement of lake-effect precipitation east of Lake Ontario and over the Tug Hill Plateau. *Mon. Wea. Rev.*, 143, 3591–3609, doi:10.1175/MWR-D-15-0009.1.

Walter, B. A., 1980: Wintertime observations of roll clouds over the Bering Sea. *Mon. Wea. Rev.* 108, 2024–2031.

Wang, C., 2005: A modelling study of the response of tropical deep convection to the increase of cloud condensational nuclei concentration: 1. Dynamics and microphysics. *J. Geophys. Res.*, 110, D21211, doi:10.1029/2004JD005720.

Warren, S. G., C. J. Hahn, J. London, R. M. Chervin, and R. L. Jenne, 1988: Global distribution of total cloud cover and cloud type amounts over the ocean. NCAR Tech. Note NCAR/TN-3171STR, 42 pp. [Available online at <http://www.atmos.washington.edu/CloudMap/Atlases/DistOcean.pdf>.]

Wegener, A., 1911: *Thermodynamik der Atmosphäre*. J. A. Barth, 331 pp.

- Wettlaufer, A., Snider, J. 2015: University of Wyoming North Redfield Hotplate Processed and Time Series Data. Version 1.0. UCAR/NCAR - Earth Observing Laboratory. <https://doi.org/10.5065/D6P26WWH>. Accessed 14 Dec 2019.
- Workoff, T. E., D. A. R. Kristovich, N. F. Laird, R. LaPlante, and D. Leins, 2012: Influence of the Lake Erie Overlake Boundary Layer on Deep Convective Storm Evolution. *Weather and Forecasting*, 27, 1279-1289, <https://doi.org/10.1175/WAF-D-11-00076.1>.
- Xiao, H., Y. Yin, L. J. Jin, Q. Chen, and J. H. Chen, 2014: Simulation of aerosol effects on orographic clouds and precipitation using WRF model with a detailed bin microphysics scheme. *Atmospheric Science Letters*, 15, 134–139.
- Yang, P., K. N. Liou, L. Bi, C. Liu, B. Q. Yi, and B. A. Baum, 2015: On the radiative properties of ice clouds: Light scattering, remote sensing, and radiation parameterization. *Adv. Atmos. Sci.*, 32, 32–63, doi:10.1007/s00376-014-0011-z.
- Yuan, T., L. A. Remer, and H. Yu, 2011: Microphysical, macrophysical and radiative signatures of volcanic aerosols in trade wind cumulus observed by the A-Train. *Atmos. Chem. Phys.*, 11, 7119–7132, doi:10.5194/acp-11-7119-2011.

**Table 1:** Weather Research and Forecasting (WRF) model parameterizations

Parameterization	Option
LW Radiation	RRTMG (Stamnes et al., 1988)
SW Radiation	RRTMG(Stamnes et al., 1988)
PBL	MYNN (Nakanishi and Niino, 2006)
Cumulus	(Domain 1) Kain–Fritsch (Kain, 2004)
Land surface	RUC LSM (Smirnova et al., 1997)

**Figures:**

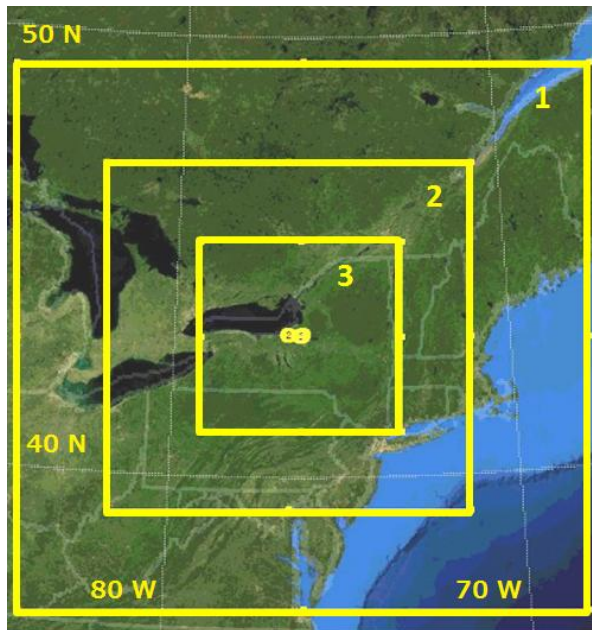


Figure 1. Model domains and terrain

# North Redfield

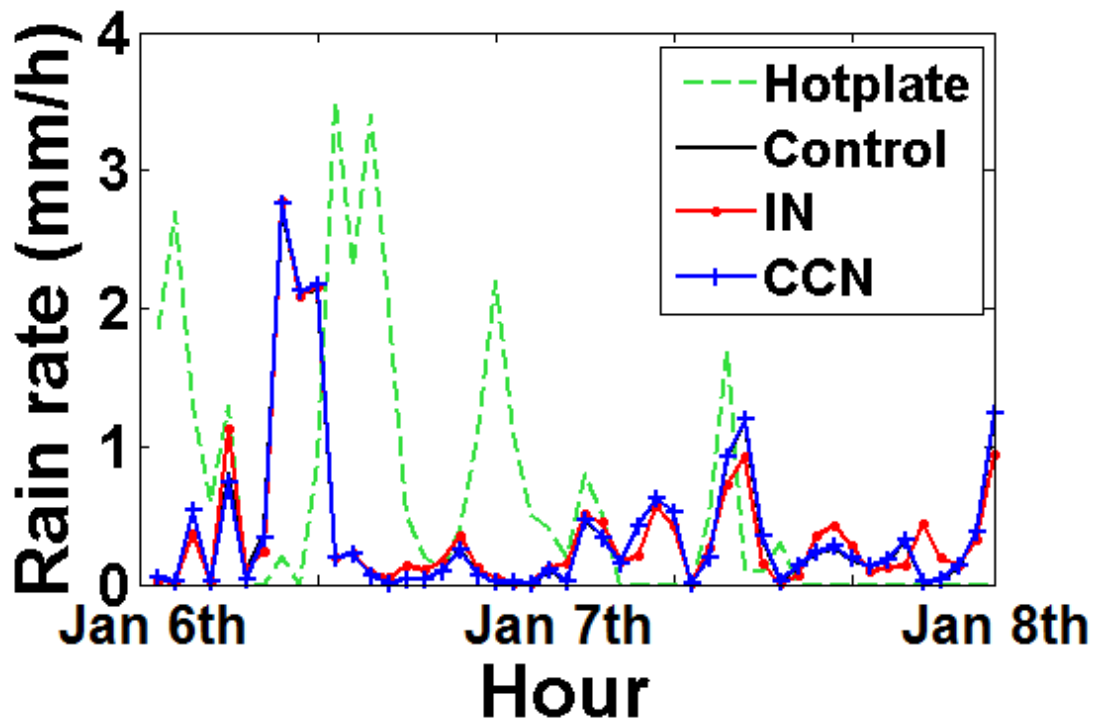


Figure 2. comparison of surface precipitation rate over North redfield (43.62E, 75.87W) between three Cases and hotplate observation

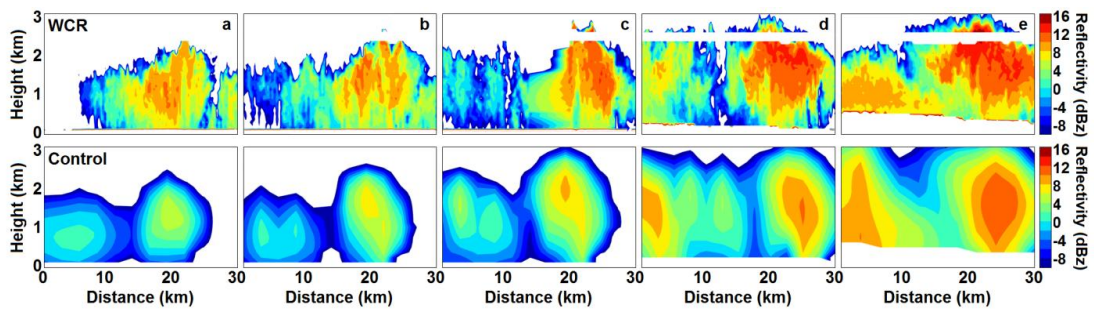


Figure 3. comparison of Wyoming cloud radar (WCR) measured (upper row) and WRF simulated (lower row) reflectivity 13:45 to 15:00 UTC, Jan 7<sup>th</sup>. 5 slices of cross-lake band measurement at (a to e) 76.8°W, 76.5°W, 76.3°W, 76°W and 75.8°W. All slices were arranged from south to north.

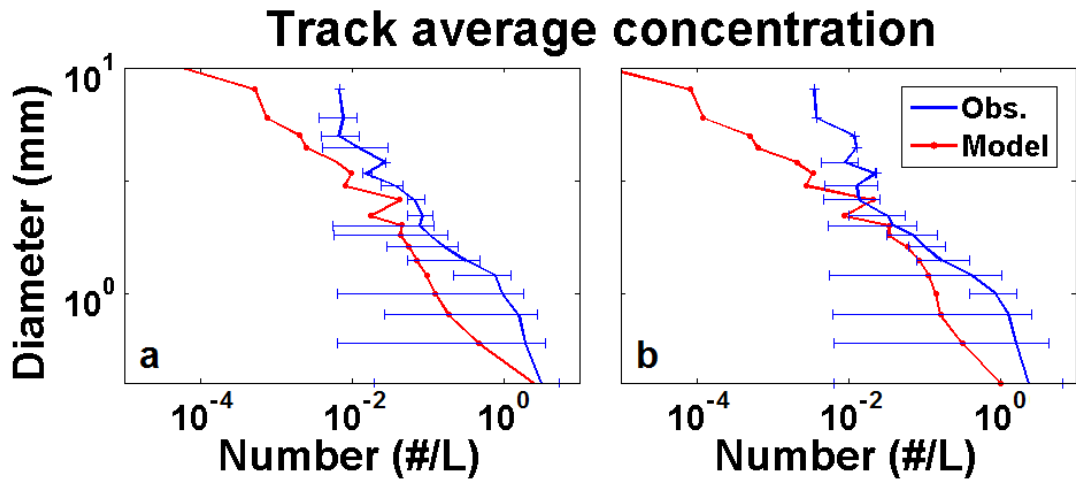


Figure 4. air-borne 2D-P PMS probe measurement (blue lines) and model simulation (red lines) of particle size distribution, averaged along the flight track at two time periods: 13:15 UTC to 16:45 UTC (left panel) and 19:15 UTC to 23:00 UTC (right panel). Blue bar indicate the range of the measurement

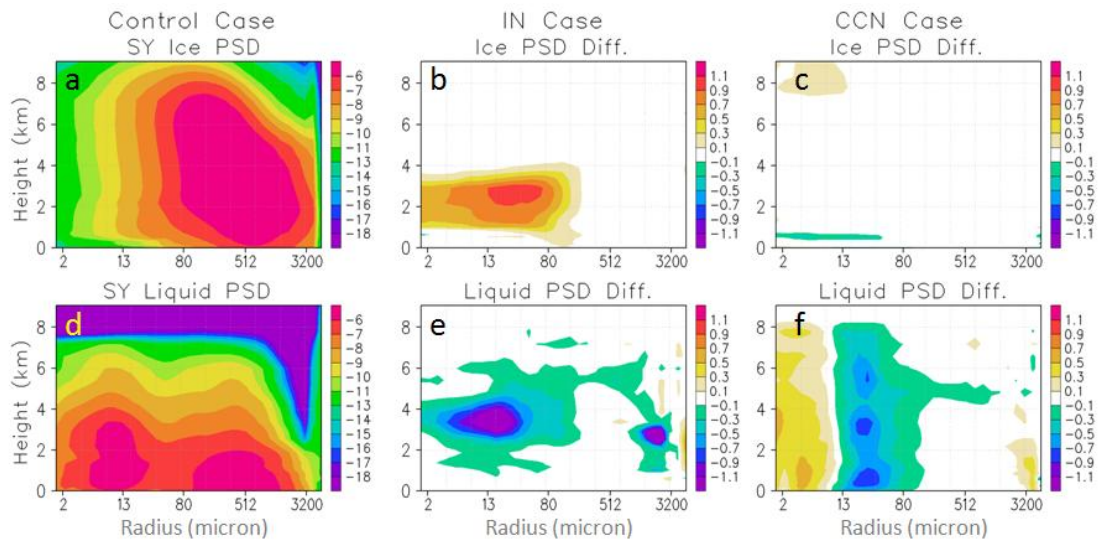


Figure 5. liquid and ice particle size distribution as a function of (melted) particle radius and height, averaged over the whole domain over the synoptic event for Control Case (first column); and the difference between IN Case (second column), CCN Case (third column) and the Control Case

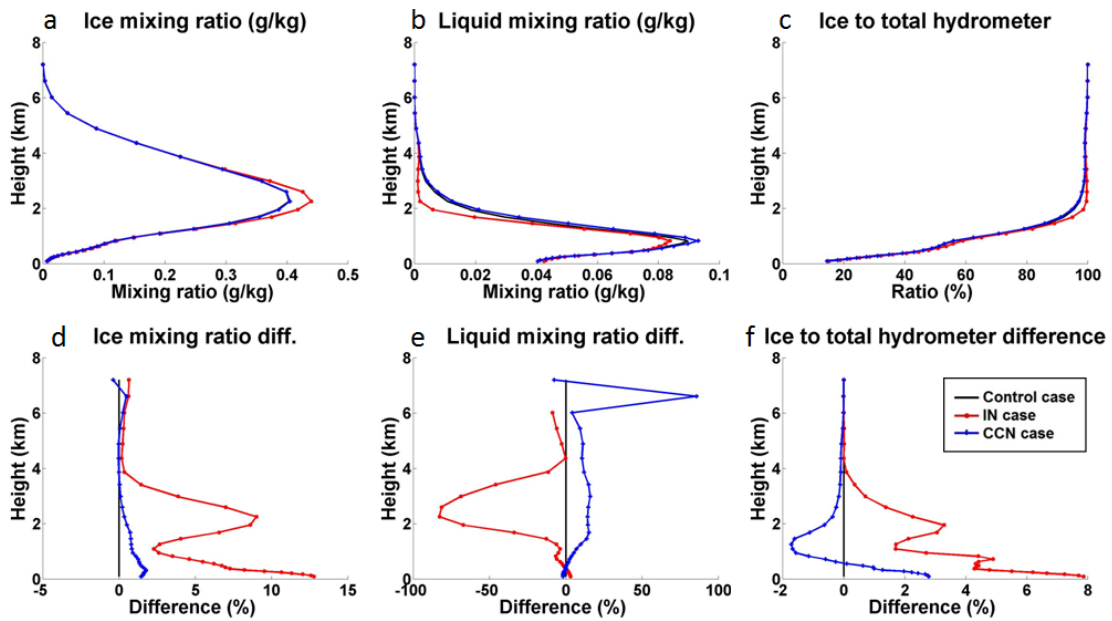


Figure 6. domain averaged ice (ice crystals and snow particles) mixing ratio, liquid (cloud droplets and rain drops) mixing ratio and ice partition in total hydrometer averaged over the synoptic event, and their difference (lower panel)

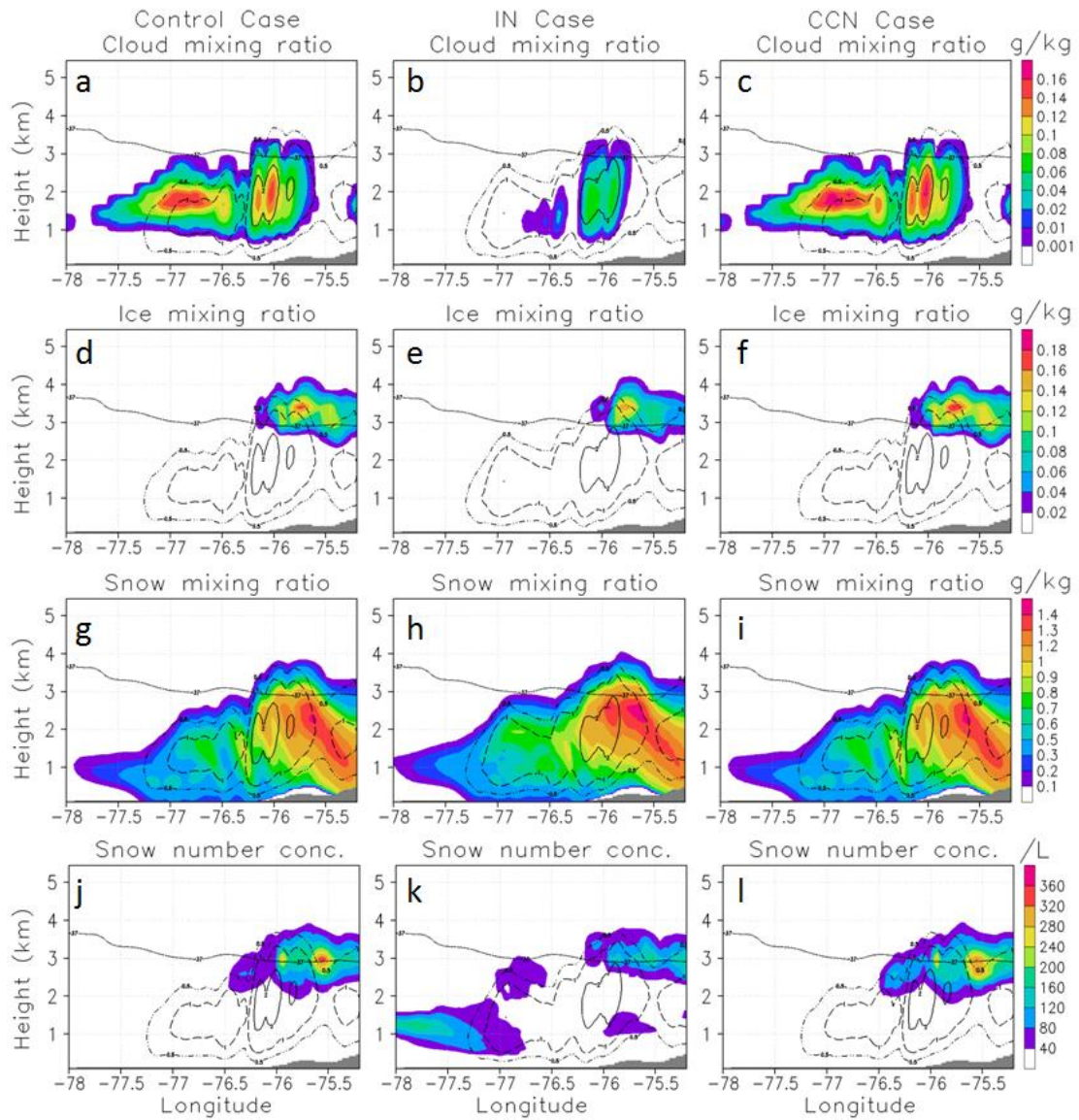


Figure 7. cloud, ice, snow mixing ratio and snow number concentration along the lake effect cloud band. Black contour indicating  $-37^{\circ}\text{C}$  level at 4 km, as well as vertical motion at 0.5 m/s (dot-dash), 1 m/s (dash) and 2 m/s (solid line). Terrain is shaded grey.

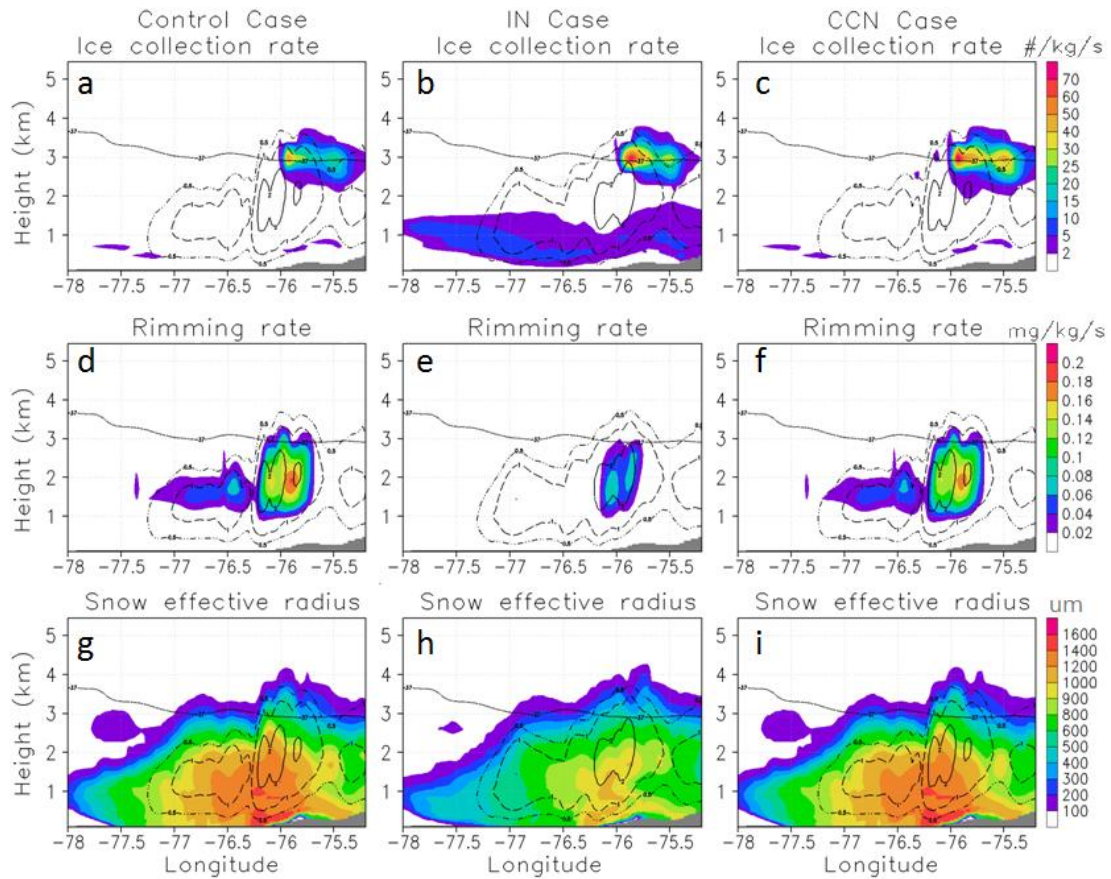


Figure 8. ice collection rate, rimming rate and snow effective radius along the cloud band. Black contour indicating  $-37\text{ }^{\circ}\text{C}$  level at 4 km, as well as vertical motion at 0.5 m/s, 1 m/s and 2 m/s. Terrain is shaded grey.

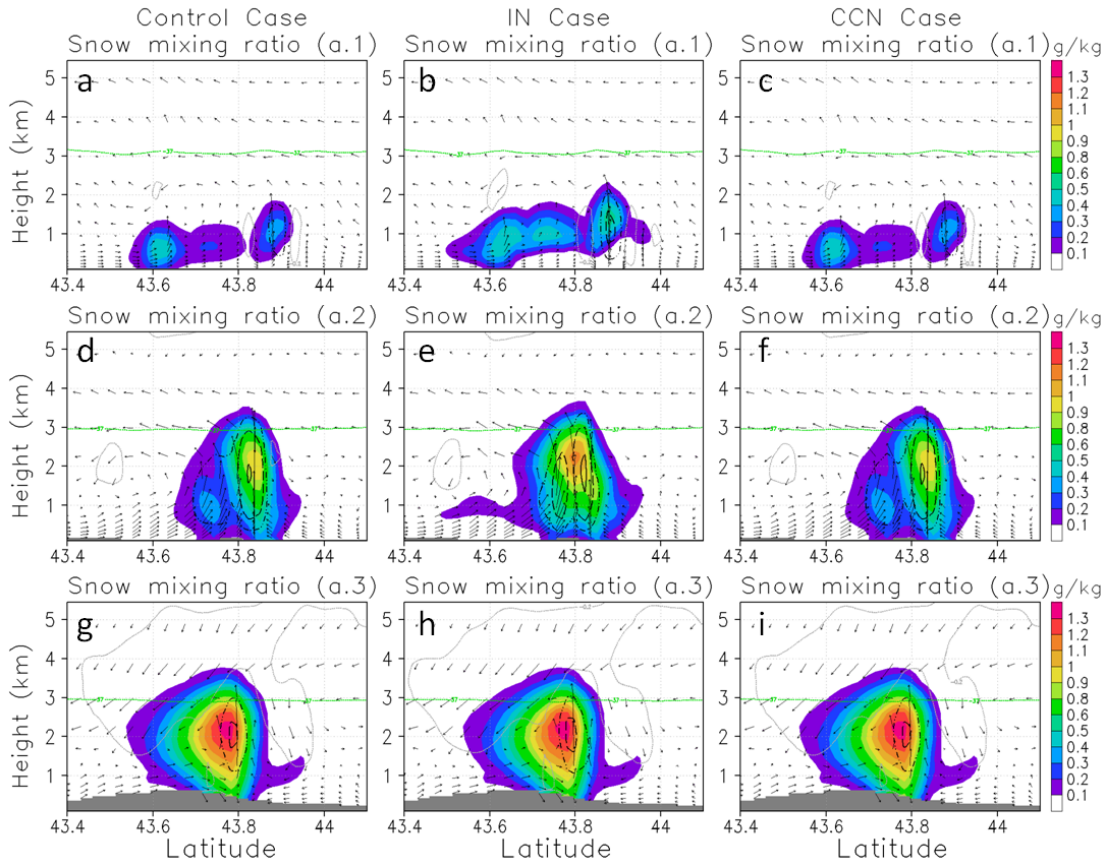


Figure 9. snow mixing ratio at three areas across the cloud band at 77 °W, 76 °W and 75.5 °W, for three cases

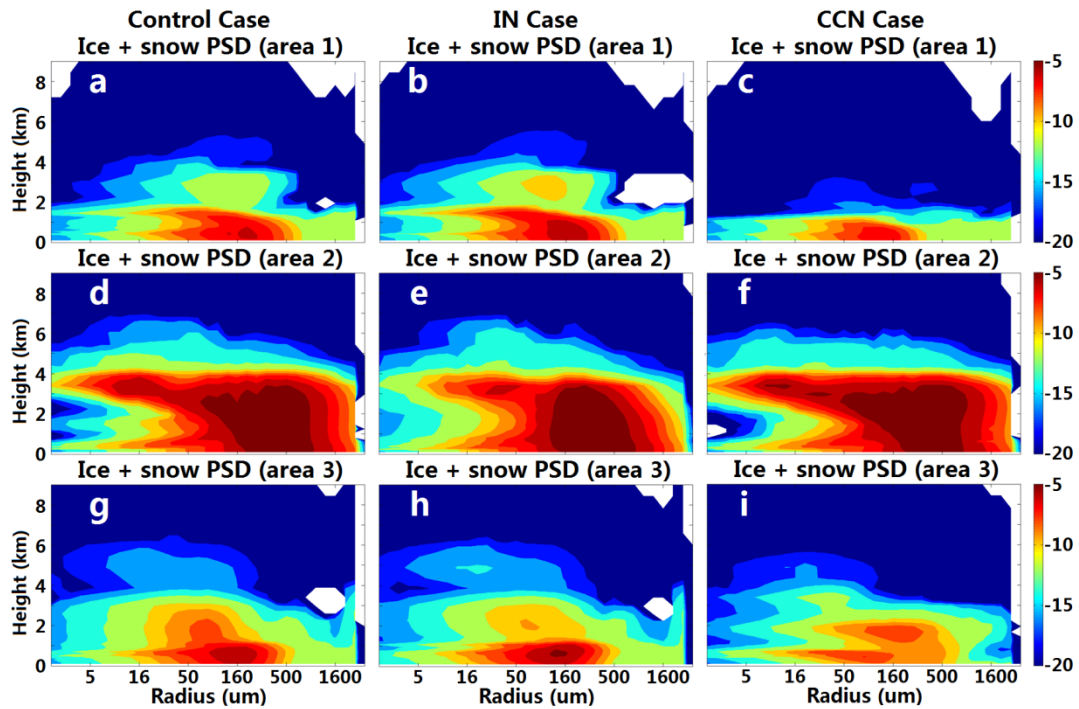


Figure 10. ice and snow particle size distribution (PSD) at the three areas same as figure 8

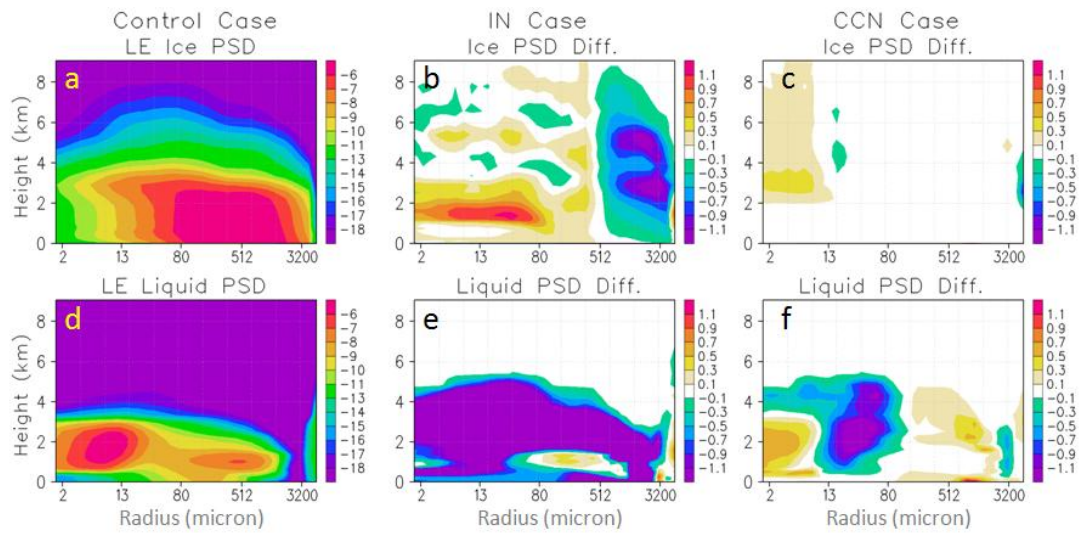


Figure 11. ice and liquid particle size distribution averaged over the whole domain over the lake effect event

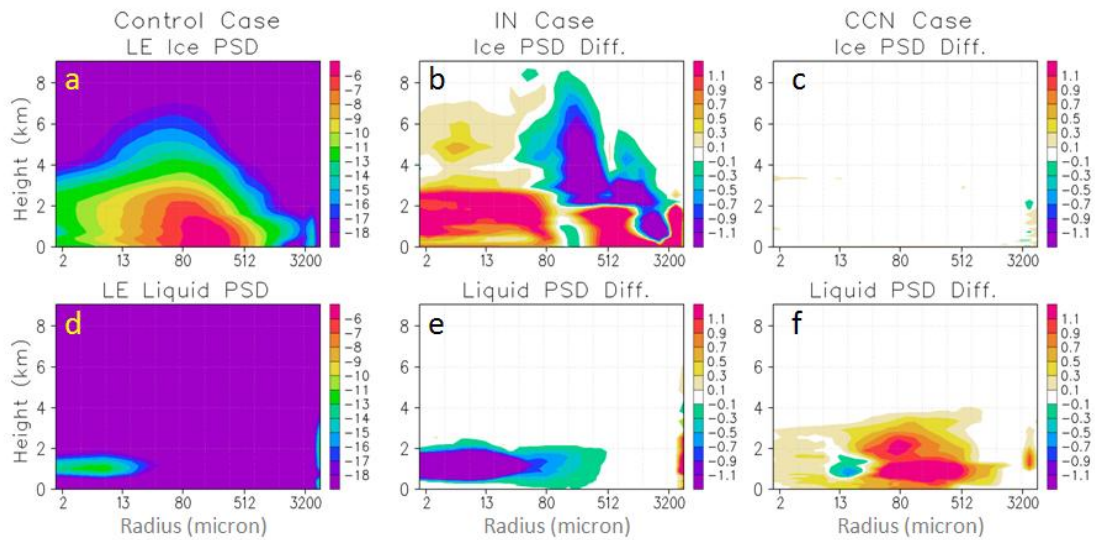


Figure 12. similar to fig.8, but for the Forest (No-Lake) Cases

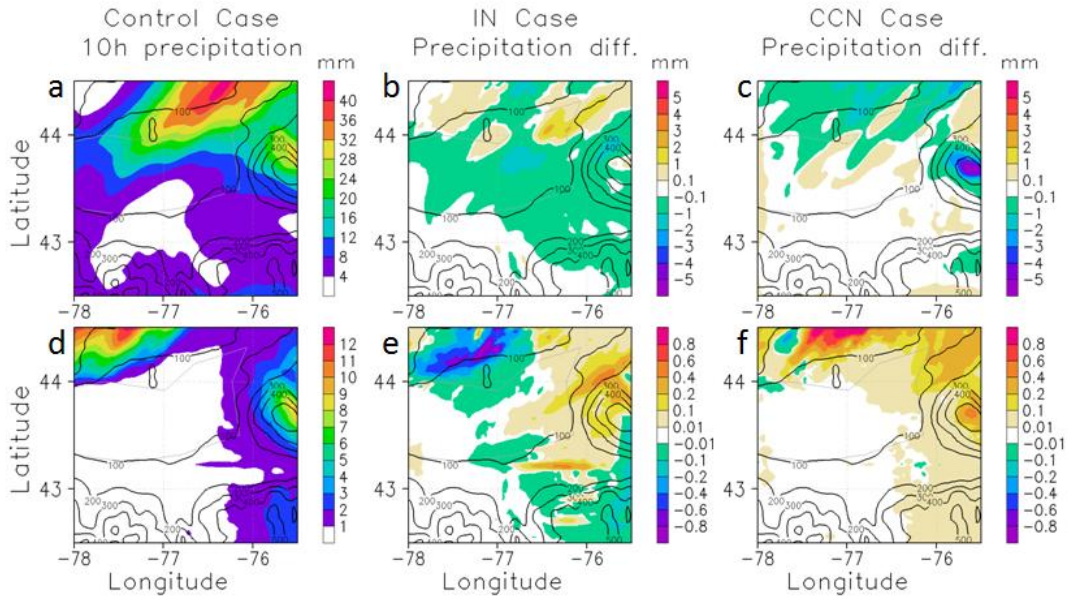


Figure 13. Surface accumulated rain (first row) and snow (second row) over domain 3 in the synoptic event

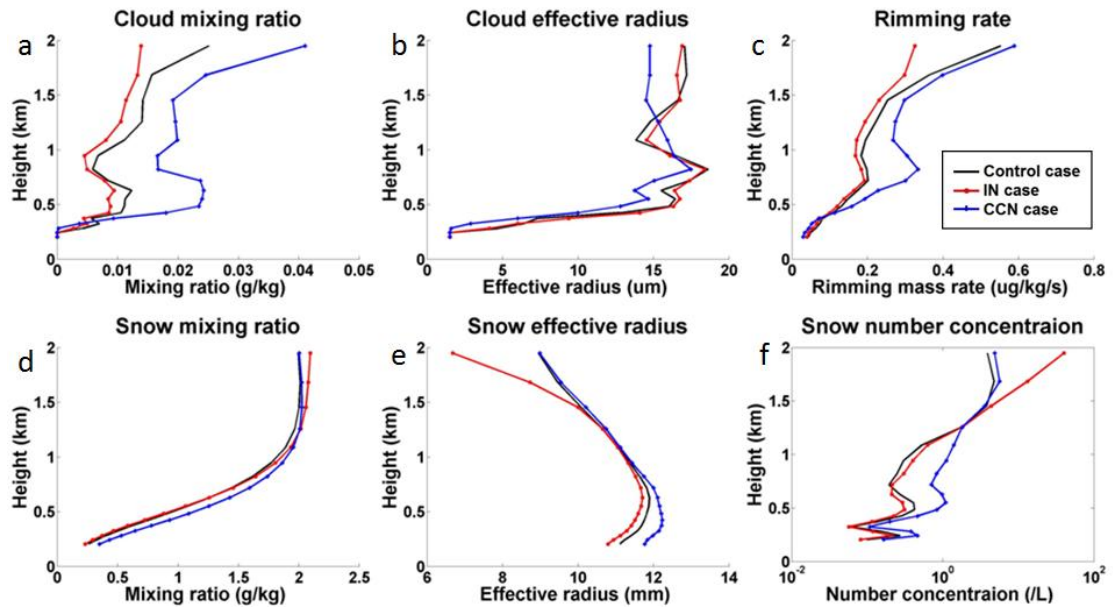


Figure 14. near surface properties at snowing area for the first precipitation peak

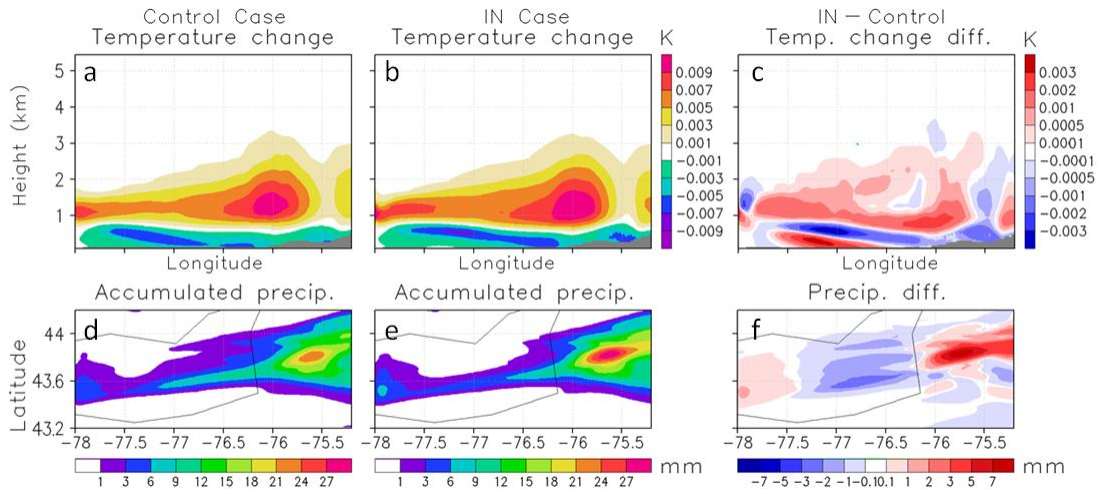


Figure 15. (first row) temperature change due to latent heat release, averaged over the lake effect event (7<sup>th</sup> 90UTC to 8<sup>th</sup> 00UTC, starting after the lake band became more stable), and (second row) snow water equivalent accumulated over the lake effect event

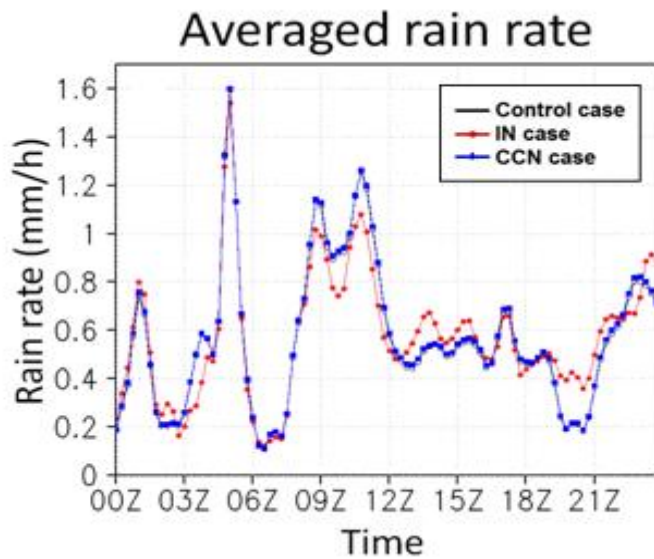


Figure 16. rain rate averaged over the Tug Hill (7<sup>th</sup> 00UTC to 8<sup>th</sup> 00UTC)